

CHANGES IN THE COASTAL MORPHOLOGY OF VRACHATI, GREECE

by
C.I. Moutzouris*
A.J. Rogan** , M. ASCE

ABSTRACT

The coastal morphology of Vrachati, which lays on the southeastern coast of the Corinthiakos Gulf, has considerably changed since the construction of two successive coastal structures. The present paper describes these changes and attempts to estimate the rate of longshore drifting sediment load. The description of the changes and the estimation of the rate are based on observations of aerial photographs of the area and on extensive bottom sediment sampling.

1. INTRODUCTION

The Corinthiakos Gulf lays between Peloponnesos and the mainland of Greece (see Fig. 1). According to Piper et al., 1980, it is a major late Cenozoic graben with maximum depth of 860m in its eastern part. It communicates with the Patraikos Gulf through the Rion Straits and with the Saronikos Gulf through the Canal of Corinthos. Beaches are coarsest and steepest where exposed to the prevailing winds.

Vrachati lays on the southern coast of the southeastern part of the Corinthiakos Gulf (see Fig. 2). The coast there has a mild slope mostly due to prodelta platforms from torrents draining into the sea and to accumulation of sediments. Cir-

* Senior Lecturer, ** Professor,
National Technical University of Athens, Civil Engineering
Department, Patission 42, Athens, Greece.

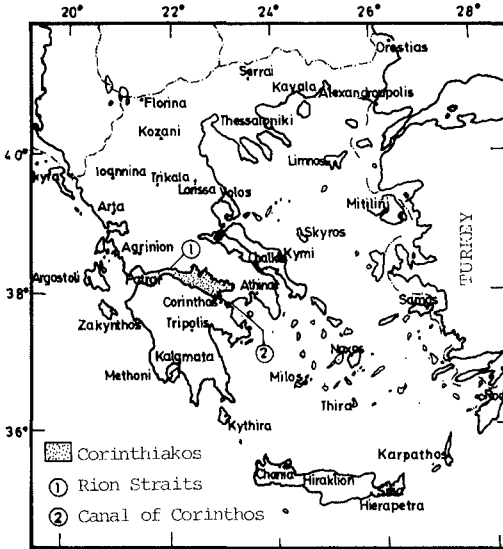


Fig. 1. -Map of Greece and the Corinthiakos Gulf

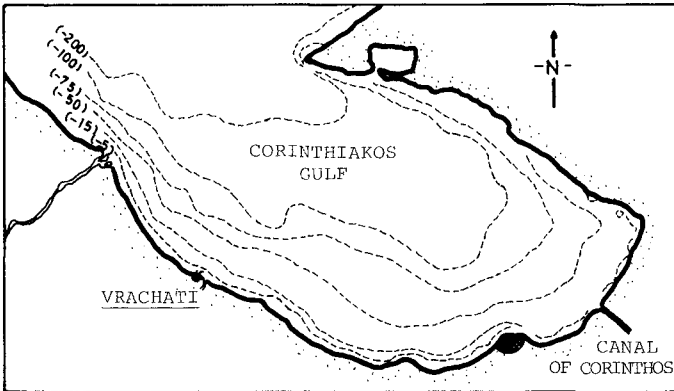


Fig. 2. -Southeastern part of the Corinthiakos Gulf

ulation is mostly wind-driven. The tidal current through the Canal of Corinthos is rather weak and does not really affect the circulation in the Vrachati coast. Mean tidal range in the area is very small, locally less than 20 cm. There is an almost bimodal wind pattern from eastern and western directions, but longshore circulation is dominated by waves and wind-driven currents mostly from the W, due to their higher frequencies of occurrence.

A breakwater was built at Vrachati in 1939 in order to provide protection to small fishing vessels. The presence of the breakwater disturbed the nearshore circulation pattern and resulted in intense modifications of the coastal morphology. For this reason, a groin was built in 1967 upstreams of the breakwater. The groin only decreased the rate of coastal modifications. Even today considerable quantities of sediments are locally deposited, as it can be seen in Fig.3.



Fig. 3. -The coast of Vrachati

The effort at the Civil Engineering Department (CED) of the National Technical University of Athens (NTUA) has focused on the nearshore processes at the southern coast of the Corinthiakos Gulf, and more specifically at the Vrachati coast, for three main reasons :

- This coast suffers from extensive erosion and accretion. Efforts are being made now to deal with this problem : the latest one is a comprehensive study which is about to be assigned by the Ministry of Public Works.
- The existence at Vrachati of the breakwater and the parallel groin combined with the simultaneous existence of aë-

rial photographs taken regularly during the same period permit the study of the evolution of the shoreline. The system of the two structures acts as a trap and allows the study of longshore drifting small-sized sediments.

The first part of the present paper describes the evolution of the shoreline at Vrachati due to the construction of the two coastal structures. Then an estimation of the rate of longshore drifting sediments is made.

2. EVOLUTION OF THE SHORELINE

The shoreline of Vrachati was straight before the construction of the breakwater, which was built in 1939 perpendicular to the shoreline (see Fig. 4). Its total length is 189 m. Intense accretion to its left and right occurred after the construction of the breakwater. The zone of accretion to the left had a length of approximately 750m. Longshore drifting sediments were deposited there, due mainly to the presence of the breakwater which was a form of littoral barrier. The zone of accretion to the right was extending up to a torrent draining to the sea and had a length of approximately 330 m. Sediments were accumulating there mainly from the torrent. A part of the load deposited there is believed to have its origins also from the longshore drifting load. The general shape of accretion around the breakwater indicates that the main direction of drift of longshore sediments past the Vrachati coast is from left to right.

In order to protect the coast from the aforementioned accretion, a groin of 135m was built in 1967 perpendicular to the shoreline at a distance of 158m to the left of the breakwater. As a result, further accretion occurred to the left of the groin, because the longshore drifting sediments were now obstructed by the new littoral barrier. The shoreline started to retreat in the zone between the two structures. This is due to the decreased quantities of longshore drifting sediments by-passing the groin and being deposited in the zone. The evolution of the shoreline to the right of the breakwater has not shown any clear tendencies. A remarkable difference between the two beaches upstreams and downstreams of the two structures is noted here : the upstream beach is made of pebbles, while the downstream beach is made of fine sand.

Long observations in-situ under wave attack conditions led the writers to the conclusion that the longshore drift of sediments is partially interrupted by the groin. The groin is a classical partial littoral barrier. Most of the suspended load by-pass the groin and are partially deposited in the zone between the groin and the breakwater and in the zone protected by the breakwater. If there were only the

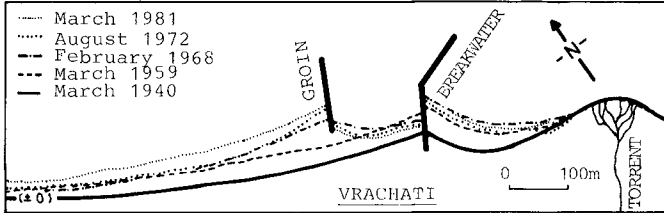


Fig. 4. -Evolution of the shoreline at Vrachati

groin, an erosion would have occurred downstream of the groin. Because of the presence of two successive structures (groin, breakwater), part of the suspended load is trapped in-between. The above qualitative observations are confirmed also by the grain-size analysis of the sediments, as it is analysed later.

3. MODEL APPLIED

It is commonplace to state that the second best method for estimating the rate of longshore drifting sediments, in cases where no data exist, is to study in detail the shoreline evolution as well as the sediments accumulated in the area. Following the above statement and according to the visual observations reported previously, the model chosen to apply for the estimation of the total rate of longshore drifting sediments was based partially on the shoreline evolution and partially on the sediment sizes (see Fig. 5). This model is somehow consistent with the Baker "two line theory" on partial transport blockage. The net total longshore drifting load S is composed of two components :

$$(1) \quad S = S_b + S_s$$

S_b is the net bedload and S_s is the net suspended load. By definition, the grains of S_s are finer than those of S_b .

The bedload is estimated according to the shoreline evolution on the upstream sides of the two structures, because the structures act as littoral barriers and the accreted shoreline has not yet reached their heads. In order to apply the Pelnard-Considère method, as presented by Bijker, 1972, two time periods have been selected :

- period_a (1939-58), when only the breakwater existed.
- period_b (1967-81), when both structures existed.

The suspended load is estimated according to the size of sand sediments, which are deposited in the zone between the two structures. This zone is a natural trap for fine grains, because of decreased current action.

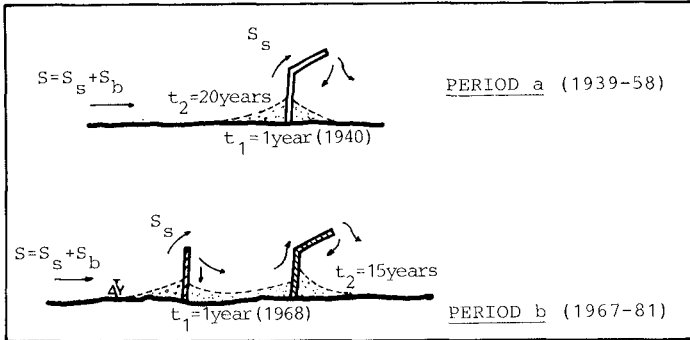


Fig. 5.- Model applied for the estimation of S

4. TECHNIQUES USED

The following techniques have been used for the application of the model : analysis of successive aerial photographs, sediment sampling and analysis and wave hindcasting.

4.1. Aerial photographs

Many sequences of aerial photographs were examined. They had been taken in successive years by the Directorate of Aerial Photographing, Ministry of Regional Planning, Housing and Environment. The examination permitted to follow the shoreline evolution as function of time and presence of coastal structures.

It was found that the shoreline progressed as follows (see Fig. 5) :

$\Delta Y = 35 \text{ m}$ during period a (upstreams of the breakwater)
 $\Delta Y = 27 \text{ m}$ during period b (upstreams of the groin)

4.2. Sediment sampling and analysis

Many spot samples have been collected from various locations in the surf zone along the coast, because spot samples are

usually representative of one sedimentation unit (see Fig. 6). For comparison reasons, some of the samples have been collected from on-shore. In order to check the influence of the changing wave climate, samples have also been collected in summer and autumn times.

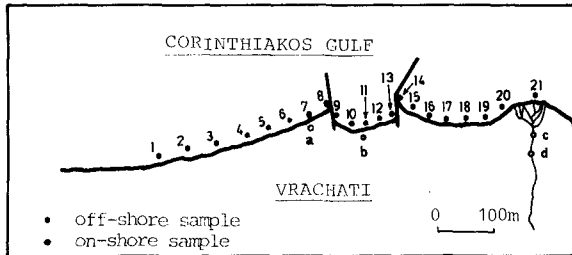


Fig. 6.- Sites of sampling along the coast

The samples were prepared for grain-size analysis and then analysed in the laboratory of the Chair of Foundations, CED/NTUA. Size distribution was determined by standard sieve analysis techniques. The size analysis data were plotted as cumulative curves with arithmetic ordinate, which is a commonly used method of graphic presentation (see Constantiniadis and Mavromatos, 1982, and Markoulidis and Zissis, 1983). The material was found to range mainly from fine sand to gravel. The particle sizes and statistical parameters of the samples were found to change along the coast. The grain-size cumulative curves may be classified into 5 families :

Samples 1, 2, 3, 4, 5, 6, 7 (see Fig. 7)

They are coarse grained because they come from the exposed coast upstreams of the structures. Large quantities of the material existed there even before the erection of the structures : particles with diametres as big as 40mm cannot be transported by wave-induced currents. The population of these samples characterises most of the exposed beaches of Corinthiakos : it is a poorly sorted beach with strongly fine-skewed and mesokurtic population.

Samples 8, a, b (see Fig. 7)

They are characteristically bi-modal, because fine grains were trapped by the groin. Curve 8 is met in almost every samples from the zone upstreams of a littoral barrier.

Samples 9, 10, 11, 12, 13 (see Fig. 7)

They are fine grained because of extensive accretion in this area of reduced wave and current action. They characterize a moderately sorted beach with coarse-skewed and leptokurtic population.

Samples 14, 15, 16, 17, 18, 19, 20 (see Fig. 8)

They range from fine-grained (in the protected zone) to median-grained (in the zone of restored current action). Samples 14 and 15 are well sorted with coarse-skewed and platykurtic population.

Samples 21, C, d (see Fig. 8)

They are very coarse-grained, due to the contribution of the torrent.

No significant seasonal change has been detected in the size distribution curves of the samples, especially in the protected zones (see Fig. 9).

4.3. Wave hindcasting

Wave data do not exist in the area under examination. For this reason wave characteristics in deep sea were computed according to the SMB method. Wind data are regularly taken in the area by the National Meteorological Service (EMY). Annual frequencies of occurrence of winds, which generate waves in the Vrachati area, are shown in Table 1. The effective fetch F_{ef} from these directions and the corresponding wave heights H_o and periods T are given in Table 2.

Refraction diagrams for the most frequent waves from E, NE, N and NW were computed according to a numerical method used at the Chatou Research Center-CREC (see Lepetit, 1964). According to this method the refraction coefficient is analysed in two partial coefficients. The first is related to the variation of distance between the orthogonals. The second depends on the modification of the phase velocity. The data introduced for the numerical analysis of the differential equation were the bottom topography, the deep sea characteristics of the monochromatic waves and the phase velocity of the waves. The equation was solved numerically by computer (see Petridis, 1982). Resulting refraction diagrams for waves from E and NE are shown in Fig. 10.

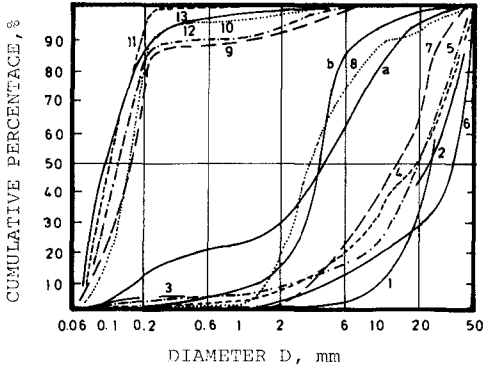


Fig. 7.- Grain-size cumulative curves

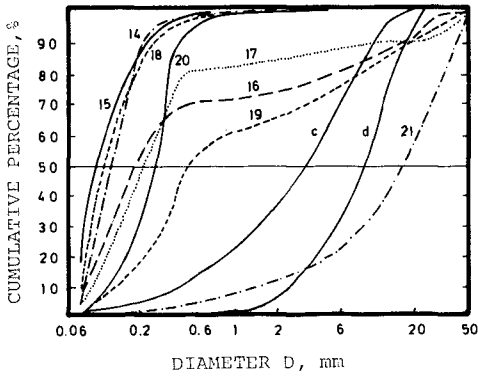


Fig. 8.- Grain-size cumulative curves

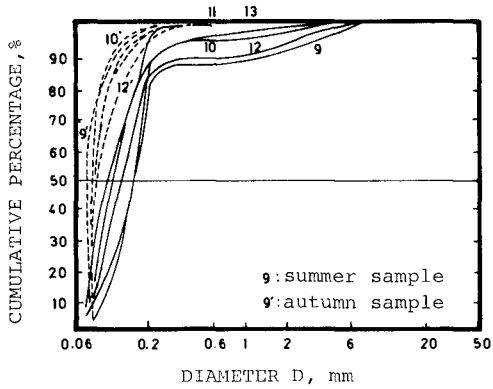


Fig. 9.- Grain-size cumulative curves as function of seasons

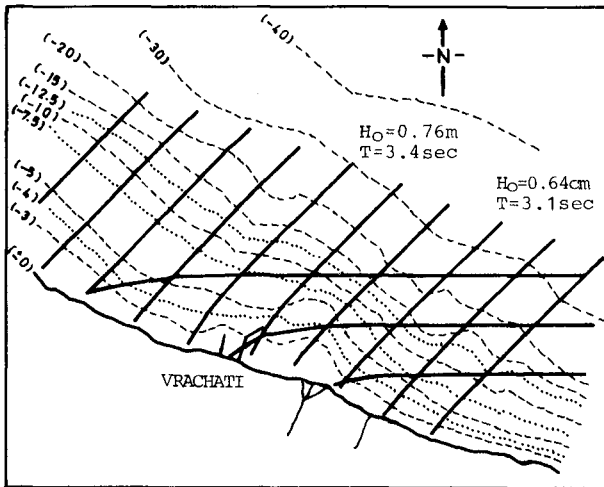


Fig. 10.- Refraction diagrams for waves E and NE

| WIND Beaufort | NW | N | NE | N |
|------------------|------|------|------|-----|
| 4 | 3.2 | 1.9 | 0.5 | 0.4 |
| 5 | 1.4 | 1.2 | 0.4 | 0.7 |
| 6 | 0.4 | 0.4 | 0.3 | - |
| 7 | 0.02 | 0.04 | 0.03 | - |
| 8 | - | - | 0.01 | - |
| TOTAL | 5.02 | 3.54 | 1.24 | 1.1 |

Table 1.- Annual frequency (%) of occurrence of off-shore winds (data from EMY)

| WIND | | NW | | | N | | |
|----------|---------|--------------------|--------------|------------|--------------------|--------------|------------|
| Beaufort | (knots) | F_{ef} (n.m.) | H_o (m) | T (sec) | F_{ef} (n.m.) | H_o (m) | T (sec) |
| 4 | 13 | 9.8 | 0.51 | 2.8 | 14.82 | 0.58 | 2.1 |
| 5 | 19 | | 0.82 | 3.5 | | 0.91 | 3.4 |
| 6 | 24 | | 1.06 | 4.0 | | 1.25 | 3.8 |
| 7 | 30 | | 1.4 | 4.5 | | 1.65 | 4.4 |
| 8 | 37 | | - | - | | - | - |
| WIND | | NE | | | E | | |
| Beaufort | (knots) | F_{ef} (n.m.) | H_o (m) | T (sec) | F_{ef} (n.m.) | H_o (m) | T (sec) |
| 4 | 13 | 7.98 | 0.46 | 2.7 | 4.62 | 0.41 | 2.5 |
| 5 | 19 | | 0.76 | 3.4 | | 0.64 | 3.1 |
| 6 | 24 | | 0.98 | 3.8 | | 0.85 | 3.5 |
| 7 | 30 | | 1.28 | 4.4 | | 1.13 | 4.0 |
| 8 | 37 | | 1.65 | 4.9 | | - | - |

Table 2.- Wave characteristics in deep sea at the Vrachati area

5. RESULTS

5.1. Bedload

The net load S_b was evaluated from the measured progression ΔY of the shoreline during a certain number of years. According to results reported earlier, the shoreline progressed 35m in 19 years (period a) and 27m in 14 years (period b). Surveys made in-situ indicated that the depth of active

sediment transport h is of the order of only 3m.

The angle of incidence α of each monochromatic wave is defined as the angle between the wavecrests and the shoreline. α_0 is the value of α in deep sea. The average angles $\bar{\alpha}_d$ of wave incidence from each direction at the depth contour of -3m were evaluated from the refraction computations and are presented in Table 3. Positive (negative) values of $\bar{\alpha}_d$ indicate incidence from the left (right) to the right (left) of Fig. 4. The average angle $\bar{\alpha}$ of wave incidence from all directions at the depth contour of -3m was evaluated according to the frequencies of occurrence of Table 1. $\bar{\alpha}$ was found equal to $+1.21^\circ$.

| DIRECTION | FREQUENCY | $\bar{\alpha}_0$ ($^\circ$) | $\bar{\alpha}_d$ ($^\circ$) |
|-----------|-----------|----------------------------------|----------------------------------|
| NW | 0.0502 | +67.5 $^\circ$ | +33.50 |
| N | 0.0354 | +22.5 $^\circ$ | +12.92 |
| NE | 0.0124 | -22.5 $^\circ$ | -21.38 |
| E | 0.0110 | -67.5 $^\circ$ | -60.00 |

Table 3.- Average angles of wave incidence at -3m

After introducing the above values to the equations of Pel-nard-Considère, it was found that :

$$S_b = 36.5 \times 10^3 \text{ m}^3/\text{year} \quad \text{during period a}$$

$$S_b = 31.8 \times 10^3 \text{ m}^3/\text{year} \quad \text{during period b}$$

As it can be seen S_b was higher in period a than in period b, due to the obstruction from the groin.

The above method of estimation of S_b has several weak points. But it is undeniable that most existing data of longshore drifting sediments quantities have been gathered from surveys of the accumulated material in littoral barriers (Brun, 1976).

For comparison reasons, S_b was next computed according to a second method. In a very recent paper Hallermeier, 1982, proposed a method of computation of bedload, which accounts for the sediment sizes, the bottom slope and configuration, the wave diffraction, etc. According to this approach, S_b depends upon some characteristic parameters : the wave height H_e , length L_e and angle α_e at the seaward limit to littoral zone, the water depth d_e at the same limit, the parameter $\Theta (=d_e/H_e)$, the median sediment grain diameter M_D , the wave reflexion and the bottom angle. Table 4 presents the analytical computations of S_b according to Hallermeier for each monochromatic wave given in Table 2. Local surveys indicated that the average bottom angle in the area is of

| WIND | f | T (sec) | d _e (m) | H _e (m) | L _e (m) | θ | α _e (°) | Q (m ³ /yr) |
|------|--------|------------|-----------------------|-----------------------|-----------------------|-------|-----------------------|---------------------------|
| NW | 0.032 | 2.8 | 0.92 | 0.490 | 7.76 | 0.533 | 29.34 | 14668.7 |
| | 0.014 | 3.5 | 1.48 | 0.786 | 12.28 | 0.531 | 30.46 | 17641.6 |
| | 0.004 | 4.0 | 1.91 | 1.018 | 15.92 | 0.533 | 31.32 | 8535.4 |
| | 0.0002 | 4.5 | 2.50 | 1.339 | 20.44 | 0.535 | 32.50 | 768.6 |
| N | 0.019 | 2.1 | 1.21 | 0.538 | 8.28 | 0.445 | 10.956 | 6449.8 |
| | 0.012 | 3.4 | 1.57 | 0.861 | 12.12 | 0.548 | 11.352 | 5531.3 |
| | 0.004 | 3.8 | 2.11 | 1.173 | 15.55 | 0.556 | 11.946 | 3540.1 |
| | 0.0004 | 4.4 | 2.80 | 1.550 | 20.80 | 0.554 | 12.705 | 668.9 |
| NE | 0.005 | 2.7 | 0.84 | 0.443 | 7.14 | 0.528 | -20.025 | 1237.7 |
| | 0.004 | 3.4 | 1.37 | 0.73 | 11.46 | 0.533 | -20.356 | 2688.6 |
| | 0.003 | 3.8 | 1.76 | 0.938 | 14.50 | 0.533 | -20.6 | 3423.3 |
| | 0.0003 | 4.4 | 2.31 | 1.228 | 19.25 | 0.532 | -20.944 | 595.7 |
| | 0.0001 | 4.9 | 2.94 | 1.50 | 24.10 | 0.537 | -21.338 | 289.9 |
| E | 0.004 | 2.5 | 0.74 | 0.394 | 6.19 | 0.532 | -50.583 | 1449.0 |
| | 0.007 | 3.1 | 1.15 | 0.614 | 9.54 | 0.534 | -52.292 | 5793.6 |

Table 4.- Computation of bedload according to the Hallermeier equation

the order of 2°. The corresponding average wave reflexion coefficient is of the order of 3%. For the evaluation of the median diameter it was considered that the samples 18, 19 and 20 are the most representative : their grain-size cumulative curves agree well with the corresponding curves of samples from undisturbed areas. For this reason, M_D was taken equal to 0.3mm.

According to the computations in Table 4 the gross loads are as follows :

$$S_b^{\leftarrow} = 57.8 \times 10^3 \text{ m}^3/\text{year} \quad \text{from left to right}$$

$$S_b^{\rightarrow} = 15.5 \times 10^3 \text{ m}^3/\text{year} \quad \text{from right to left}$$

The net bedload is :

$$S_b = 42.3 \times 10^3 \text{ m}^3/\text{year} \quad \text{from left to right}$$

The load according to Hallermeier apparently represents the net bedload during the last years, because the estimation was based on recent field data.

5.2. Suspended load

For the computation of the net suspended load S_s which is transported along the coast, information was needed on the

grains trapped between the two structures. Finally it was assumed that the graphic mean diameter M_z , as defined by Folk, 1974, is representative of the diameters ensemble :

$$(4) \quad M_z = \frac{\phi_{16} + \phi_{50} + \phi_{84}}{3}$$

ϕ is the grains diameter expressed in the phi-scale. The average M_z for the samples 9, 10, 11, 12 and 13 is computed from equ. (4) and Fig. 7 :

$$(5) \quad M_z = 0.14 \text{ mm}$$

An equation proposed by the Laboratoire Central d'Hydraulique de France-LCHF was the computation of S_s (see Leclerc et al., 1976) :

$$(6) \quad S_s = K g H L T f(\alpha)$$

g is the gravitational acceleration, H and L are the wave height and length at a water depth of 15m, α_{15} is the angle of incidence at the same depth, $f(\alpha)$ is a function of the angle α_{15} . The coefficient K is given by equ. (7) :

$$(7) \quad K = 0.18 \times 10^{-5} D^{-0.5}$$

D is the grain diameter ($\leq 1 \text{ mm}$). In the present study it is considered that the average graphic mean diameter of the samples corresponds with D .

The computations of suspended loads for each monochromatic wave given in Table 2 are shown in Table 5. The gross loads are as follows :

$$S_s' = 2.2 \times 10^3 \text{ m}^3/\text{year} \quad \text{from left to right}$$

$$S_s'' = 0.7 \times 10^3 \text{ m}^3/\text{year} \quad \text{from right to left}$$

The net suspended load is :

$$S_s = 1.5 \times 10^3 \text{ m}^3/\text{year} \quad \text{from left to right}$$

5.3. Total load

The net total sediment load drifts from left to right past Vrachati and is equal to :

$$S = 38.0 \times 10^3 \text{ m}^3/\text{year} \quad \text{during period a}$$

$$S = 33.3 \times 10^3 \text{ m}^3/\text{year} \quad \text{during period b}$$

The computation of S was based on a wide range of data : wind, sediment, bottom and shoreline progression data. The difference between period a and b is due to the different

| WIND | f | H _o (m) | T (sec) | L _o (m) | f(α) | Q (m ³ /yr) |
|------|--------|-----------------------|------------|-----------------------|------|---------------------------|
| NW | 0.032 | 0.51 | 2.8 | 12.25 | 0.36 | 298.7 |
| | 0.014 | 0.82 | 3.5 | 19.14 | " | 410.3 |
| | 0.004 | 1.06 | 4.0 | 24.99 | " | 226.1 |
| | 0.0002 | 1.4 | 4.5 | 31.63 | " | 21.3 |
| N | 0.019 | 0.58 | 2.1 | 11.30 | 0.6 | 233.0 |
| | 0.012 | 0.91 | 3.4 | 18.06 | " | 596.3 |
| | 0.004 | 1.25 | 3.8 | 22.56 | " | 381.2 |
| | 0.0004 | 1.65 | 4.4 | 30.24 | " | 78.1 |
| NE | 0.005 | 0.46 | 2.7 | 11.39 | 0.6 | 62.9 |
| | 0.004 | 0.76 | 3.4 | 18.06 | " | 166.0 |
| | 0.003 | 0.98 | 3.8 | 22.56 | " | 224.1 |
| | 0.0003 | 1.28 | 4.4 | 30.24 | " | 45.4 |
| | 0.0001 | 1.65 | 4.9 | 37.51 | " | 26.9 |
| E | 0.004 | 0.41 | 2.5 | 9.82 | 0.36 | 21.5 |
| | 0.007 | 0.64 | 3.1 | 15.11 | " | 111.9 |

Table 5.- Computation of suspended load

rates of shoreline progression during these periods.

For comparison reasons S was then computed according to the well known method of the Coastal Engineering Research Center CERC, as it is presented in the Coastal Protection Manual, 1976. This method ignores the sizes of the transported sediments and the bottom slope. The rate of longshore transport is proportional to the longshore wave energy flux. In other terms, the transport depends exclusively upon the wave climate in the area. The computation of S according to this method is shown analytically in Table 6. The gross loads are as follows.

$$S^+ = 51.7 \times 10^3 \text{ m}^3/\text{year} \quad \text{from left to right}$$

$$S^- = 12.3 \times 10^3 \text{ m}^3/\text{year} \quad \text{from right to left}$$

The net load S is :

$$S = 39.4 \times 10^3 \text{ m}^3/\text{year} \quad \text{from left to right}$$

The above value refers to time periods a and b, because it was computed from wind data covering both periods.

| WIND | f | H _o (m) | Q (m ³ /yr) |
|------|--------|-----------------------|---------------------------|
| NW | 0.032 | 0.51 | 6756.7 |
| | 0.014 | 0.82 | 6990.0 |
| | 0.004 | 1.06 | 5260.0 |
| | 0.0002 | 1.40 | 527.2 |
| N | 0.019 | 0.58 | 6897.5 |
| | 0.012 | 0.91 | 13432.4 |
| | 0.004 | 1.25 | 9901.6 |
| | 0.0004 | 1.65 | 1982.2 |
| NE | 0.005 | 0.46 | 1016.8 |
| | 0.004 | 0.76 | 2854.1 |
| | 0.003 | 0.98 | 4041.6 |
| | 0.0003 | 1.28 | 788.0 |
| | 0.0001 | 1.65 | 495.5 |
| E | 0.004 | 0.41 | 489.3 |
| | 0.007 | 0.64 | 2607.4 |

Table 6.- Computation of total load according to the CERC equation

The above computed values of net longshore drifting loads are shown in Fig. 11.

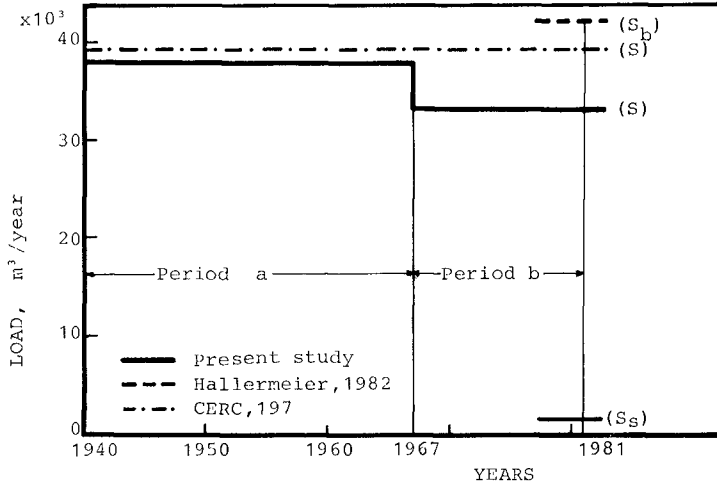


Fig.11.- Net longshore drifting load

6. CONCLUSIONS

The adopted method of estimation of the net longshore drifting load is the second best to direct measuring the load, because it is based on a wide range of data: wind, sediment, bottom, shoreline progression data. It can be applied when time presses, although many parameters are neglected. This method gives results averaged in time, while measurements of only one year or less may give very erroneous results.

The research described in the present paper will be continued with load measurements, in order to check the accuracy of the results.

7. ACKNOWLEDGMENTS

Acknowledgments are expressed to Miss Theodora Yantsi, Civil Engineer, for her assistance in the computations.

8. REFERENCES

- Bijker, E.W., 1972, "Lecture notes for topics in Coastal Engineering", Delft University of Technology, pp. 79-99.
- Bruun, P., 1976, "Port Engineering" 2nd edition, Gulf Publ. Co, Austin
- CERC, 1976, "Shore Protection Manual" U.S. Army, Corps of Engineers
- Constantinidis, D. and Mavromatos, N., 1961, "Erosion of the Corinthiakos Gulf: from Corinthos to Kiato", Diploma Thesis, Nat. Techn. Univ. of Athens, pp. 2.69-2.77 (in Greek)
- Folk, R. L., 1974, "Petrology of Sedimentary Rocks", Hemphill Publ. Co, Austin
- Hallermeier, R.J., 1982, "Bedload and wave thrust computations of alongshore sand transport", Journal of Geophysical Research, Vol. 87, No C8, July 20, pp. 5741-5751
- Leclerc, J.P., Bellessort, B. et Mignot, C., 1976, "Action de la houle sur les sédiments", Laboratoire Central d'Hydraulique de France (LCHF), pp. 143-144
- Lepetit, J.P., 1964, "Etude de la réfraction de la houle monochromatique par le calcul numérique", Bulletin du CREC, No 9
- Markoulidis, P. and Zissis, J., 1983, "Investigation of sediments flow and creation of a harbour in the area of Vrachati", Diploma Thesis, National University of Athens (to

appear, in Greek)

Petridis, P., 1982, "Refraction of sea waves", Diploma Thesis, National Technical University of Athens, pp. 161-162 (in Greek)

Piper, D.J.W., Kontopoulos, N., and Panagos, A.G., 1980, "Deltaic coastal and shallow marine sediments of the western Gulf of Corinth", *Thalassographica*, Vol. 2, No 3, pp.5-14

Rogan, A.J. and Moutzouris, C.I., 1981, "Erosion and accretion of Greek coasts caused by harbour and coastal works", *Proceedings of the 25th Congress of IANAC*, Vol. 5, Edinburgh, pp. 799-806